PAPER

Check for updates

Innovative chromene-based disperse dyes for concurrent dyeing: molecular docking, biochemical assessment, and repellent efficacy against *Culex pipiens* mosquitoes

Mohamed S. A. El-Gaby,[a] M. A. Habib,[b] Nadeem Raza,[b] Ahmed B. M. Ibrahim,[b] Ali A. Ali, [ID] *[a] Walid E. Elgammal, [ID] [a] Ahmed H. Halawa,[a] Mostafa A. Ismail,[c] Tharwat A. Selim,[d] Ahmed I. Hasaballah,[d] Mohamed A. M. El-Tabakh[d] and Gameel A. M. Elhagali[a]

Integrating a heterocyclic component into the azo dye framework substantially improves the bioactivity of the synthesized compounds. This structural modification facilitates the optimization of drug-like molecules for diverse biological and pharmacological applications. A synthetic route was adopted in this study to develop the target compounds, specifically the *4H*-chromene containing azo benzophenones **6a–d**, and their behavior on polyester fabrics was examined by optimizing the dyeing conditions. An increase in the color strength of the dyed polyester fabrics was observed with rising dyeing temperatures (100–130 °C) and prolonged dyeing durations (15–60 min). These results imply that synthetic dyes are viable options for adding a wide range of colors to polyester fabrics. In addition to their dyeing performance, bioassay evaluations demonstrated that dyes **6a–d** possess repellent efficacy against the mosquito vector *Culex pipiens*. Compound **6a** exhibited the highest repellent activity, reaching approximately 60% after 30 minutes of treatment and maintaining effectiveness for two hours, with a slight decline to 56%. In contrast, compounds **6b**, **6c**, and **6d** showed repellent effects of 53–44%, 56–45%, and 35–44%, respectively. The toxicological potential of these dyes was further investigated by assessing the performance of acetylcholinesterase (AChE) along with glutathione *S*-transferase (GST) enzymes in *Culex pipiens* insects following exposure. The synthesized *4H*-chromene-based azo dyes show promise for polyester coloration and as bioactive agents with mosquito-repellent and enzyme-inhibitory effects.

1. Introduction

Undoubtedly, mosquitoes pose a significant global health threat due to their role in transmitting numerous infectious diseases. *Culex* species are considered the most prevalent in Africa and Asia and serve as the primary vectors of filariasis, with millions of cases reported worldwide in recent years.[1] *Culex pipiens* is widely distributed[2] and is a well-established vector of West Nile virus,[3] *Wuchereria bancrofti*,[4] and the virus responsible for Rift Valley fever.[5] Furthermore, several recent studies have investigated the potential role of mosquitoes in transmitting the hepatitis C virus.[6,7] Therefore, effective mosquito control is crucial for reducing the transmission of mosquito-transported diseases and protecting the health of society. A variety of strategies have been explored for mosquito control.[8–11] These include the direct application of insect repellents to the skin, clothing, or household materials, as well as the use of protective barriers such as mosquito nets and screens. However, prolonged use of commercial mosquito coils, mats, and fumigators containing chemicals such as *N,N*-diethyl-*m*-toluamide (DEET) and synthetic pyrethroids (*e.g.*, pyrethrin, allethrin, and permethrin) has been associated with adverse health effects.[12] As a safer and more sustainable alternative, researchers have investigated the use of natural materials such as fresh moringa leaves, castor oil, and mint leaves for the development of mosquito-repellent textiles. This innovation represents a promising and creative approach to enhancing the textile industry while addressing the urgent need for effective mosquito-repellent fabrics.[13]

[a] *Department of Chemistry, Faculty of Science (Boys), Al-Azhar University, Cairo 11884, Egypt. E-mail: dr_ali055@azhar.edu.eg*

[b] *Department of Chemistry, College of Science, Imam Mohammad Ibn Saud Islamic University (IMSIU), 11623 Riyadh, Saudi Arabia*

[c] *Department of Chemistry, College of Science, King Khalid University, Abha 61413, Saudi Arabia*

[d] *Department of Zoology and Entomology, Faculty of Science (boys), Al-Azhar University, Cairo 11884, Egypt*

Chromenes represent a significant class of naturally occurring molecules, encompassing diverse forms such as tocopherols, alkaloids, anthocyanins, and flavones. The chromene nucleus is recognized as an essential structural motif in the pursuit of new drug candidates.[14] Interestingly, 4H-chromenes have demonstrated an extensive variety of medicinal properties, among which are antimicrobial,[15] antifungal,[16] antiviral,[17] anticancer,[18] antitumor,[19] analgesic,[20] antioxidant,[21] anti-influenza,[22] anti-inflammatory,[23] antidiabetic,[24] anticonvulsant,[25] anticholinesterase,[26] herbicidal,[27] antituberculosis,[28] and anticoagulant features.

Pigments and azo dyes constitute two major classes of chemical colouring agents, distinguished by their broad applications throughout numerous industrial fields.[29] Among these, azo dyes hold particular importance in the textile industry, primarily owing to their characteristic nitrogen–nitrogen double bond, which is central to their chromophoric properties and functional versatility.[30] Azo dyes have historically been extensively utilized to color a diverse array of things, such as food, paper, textiles, cosmetics, pharmaceuticals, and various consumer goods.[31] The synthesis of azo compounds can be achieved through various chemical reactions.[32] These salts, typically generated through conventional diazotization reactions, readily react with diazo-coupling nucleophiles such as phenols, naphthols, or amines under low-temperature conditions in the presence of acids and salts.[33]

Benzophenone is an essential organic scaffold that functions as a flexible precursor in the generation of insecticides, pharmaceuticals, perfumes, and organic pigments.[34] Structurally, benzophenone consists of two rings of benzene connected through an inner carbonyl functional group and is commonly referred to as benzoyl benzene.[35] Numerous naturally occurring compounds incorporate the benzophenone framework, which contributes to its prevalence in medicinal chemistry owing to its diverse biological activities.[36] Naturally occurring benzophenones display diverse medicinal benefits, including antioxidant, antifungal, anti-HIV, and antibacterial, along with antiviral effects.[37] In agriculture, the benzophenone nucleus

is of particular importance, as it constitutes the core structure of certain fungicides, such as flumorph.[38] In addition, several benzophenone-based compounds are commercially available as pharmaceuticals and sunscreens (Fig. 1). For example, ketoprofen is a powerful nonsteroidal anti-inflammatory substance with both antipyretic and analgesic actions.[39] Tolcapone, a dihydroxy benzophenone derivative, is employed in the management of Parkinson's disease,[40] while fenofibrate (Tricor) is commonly prescribed to reduce cholesterol levels in patients at risk of cardiovascular disorders.[41] Beyond therapeutic applications, benzophenones are extensively utilized as photosensitizers and constitute one of the more significant categories of materials in photochemistry. In sun protection products, they serve as UV-A/B filters, with 2-hydroxybenzophenones such as oxybenzone and sulisobenzone widely employed to prevent the penetration of harmful ultraviolet radiation into the skin.[42]

As part of our continuing investigation on the incorporation of heterocyclic constituents into azo colorant architectures,[19,43–49] we have planned and generated a new class of disperse dyes by integrating a benzophenone fragment conjugated with a 4H-chromene core. The target disperse dyes **6a–d** were obtained through the cyclocondensation of compound **4** with arylidene-malononitriles **5** in ethanol under reflux using piperidine as a catalyst. Comprehensive characterization of the synthesized compounds was performed using a combination of analytical and spectroscopic techniques. Owing to their remarkable biological characteristics, benzophenone-based azo dyes have gained significant attention for applications in diverse fields, particularly in printing and biomedicine. When applied to polyester fabrics, the synthesized dyes produced shades ranging from 1 to 5 using dyeing settings at temperatures between 100 and 130 °C and pH values of 2, 4, 6, and 8. Bioassay evaluations revealed that dyes **6a–d** exhibit repellent impact towards the mosquito vector *Culex pipiens*. Among them, compound **6a** exhibited the strongest repellent effect, while compound **6d** showed the weakest. To gain deeper insight into their biological potential, the actions of glutathione S-transferase
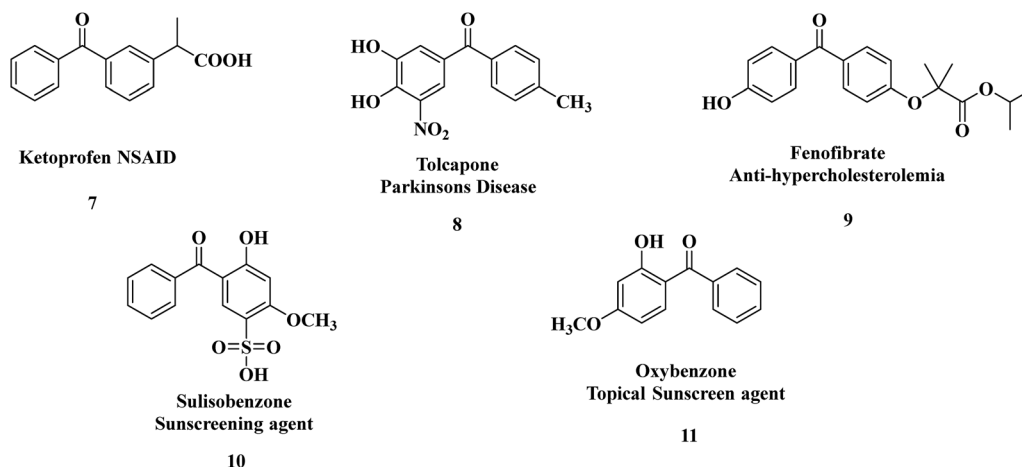

Fig. 1 Representative example of benzophenone drugs.

(GST) and acetylcholinesterase (AChE) were assessed in *Culex pipiens* larvae after exposure to these dyes. Molecular docking studies validated the adopted protocol and revealed that compounds **6a–d** displayed stronger binding affinities than the reference ligands, with compound **6a** being the most effective against AChE and compound **6d** against GST. Taken together, these findings highlight the potential of the synthesized disperse dyes not only as efficient colorants for polyester fabrics but also as promising bioactive agents with mosquito-repellent properties.

2. Experimental

2.1. Materials and instruments

The SI provides detailed information on the instruments and chemical reagents employed for the characterization of the generated molecules. The starting materials, including *para*-aminobenzophenone and *m*-dihydroxybenzene (resorcinol), were provided by Sigma-Aldrich. Sodium nitrite ($NaNO_2$), sodium acetate trihydrate ($CH_3COONa\cdot3H_2O$), sodium carbonate (purchased from Alpha Chemika, India), and concentrated hydrochloric acid (HCl) were obtained from a variety of sources, including CDH (Central Drug House) and SD Fine. Lobachem provided organic solvents, including glacial acetic acid and ethanol, without any additional purification. Using pre-coated silica gel aluminum plates (Macherey-Nagel) and DCM : MeOH (95% : 5%) as the eluting solution, we performed thin layer chromatography (TLC) analysis. We used UV light (254 nm) to observe and visualize the reactions. The 100% polyester fabric (140 gm m^{-2}, plain weave, Yarn 48 × 150 denier, the threads are 110 × 80 warp in weft, width: 66 inches, and thickness: 0.39 mm cm^{-1}) was supplied by El-Nahawy Textile Company, Egypt.

2.1.1. General procedure for the synthesis of chromenes 6a–d. Method 1: after dissolving compound **4** (0.01 mmol) in 30 mL of ethanol containing piperidine (0.1 mL), arylidene malononitrile **5** was added. The reaction mixture was refluxed for 30 minutes, and the resulting solid was filtered, washed with water, and purified by recrystallization using a suitable solvent.

Method 2: a solution of compound **4** (0.01 mmol) in ethanol (30 ml) containing piperidine (0.1 ml) was treated with a mixture of aromatic aldehyde (0.01 mmol) and malononitrile (0.01 mmol). The reaction mixture was refluxed for 30 minutes, and the resulting solid was collected by filtration, washed with water, and recrystallized from the appropriate solvent.

2.1.2. (*E*)-2-Amino-6-((4-benzoylphenyl)diazenyl)-4-(4-chlorophenyl)-7-hydroxy-4*H*-chromene-3-carbonitrile 6a. Orange colour solid (1,4-dioxane), yield 86%, m.p. 256–257 °C, FT-IR (KBr, ν_{max}/cm^{-1}); 3383, 3326, 3197 (OH/NH$_2$), 3062 (Arom-CH), 2201 (CN), 1642 (C=O), and 1593 (N=N). ^{1}H NMR (300 MHz, DMSO-d_6, δ ppm): 12.11 (s, 1H, OH, exchangeable by D$_2$O), 8.13 (d, *J* = 8.5 Hz, 2H, AB-system), 7.89 (d, *J* = 8.6 Hz, 2H, AB-system), 7.82 (s, 1H, resorcinol-H), 7.81–7.75 (m, 2H, phenyl group), 7.75–7.67 (m, 1H, phenyl group), 7.59 (t, *J* = 7.7 Hz, 2H, phenyl group), 7.39 (d, *J* = 8.4 Hz, 2H, AB-system), 7.24 (d, *J* = 8.5 Hz, 2H, AB-system), 7.14 (s, 2H, NH$_2$, exchangeable by D$_2$O), 6.83 (d, *J* = 9.0 Hz, 1H, resorcinol-H), 4.81 (s, 1H, pyrane-H). ^{13}C NMR (101 MHz, DMSO-d_6, δ ppm): 195.57, 159.94, 154.46, 153.44, 153.31, 144.45, 138.81, 137.30, 135.72, 133.39, 131.72, 131.33, 130.11, 129.61, 129.14, 128.95, 124.56, 123.01, 120.45, 112.57, 109.23, 57.20, 36.50. MS (*m/z*): 506 (M$^+$, 21.98%). Anal. calcd for C$_{29}$H$_{19}$ClN$_4$O$_3$ (506.11): C, 68.71; H, 3.78; N, 11.05; found: C, 68.59; H, 3.69; N, 10.92%.

2.1.3. (*E*)-2-Amino-6-((4-benzoylphenyl)diazenyl)-4-(4-bromophenyl)-7-hydroxy-4*H*-chromene-3-carbonitrile 6b. Red colour solid (1,4-dioxane), yield 84%, m.p. 272–273 °C, FT-IR (KBr, ν_{max}/cm^{-1}); 3375, 3311, 3195 (OH/NH$_2$), 3052 (Arom-CH), 2202 (CN), 1644 (C=O), and 1593 (N=N). ^{1}H NMR (300 MHz, DMSO-d_6, δ ppm): 12.12 (s, 1H, OH, exchangeable by D$_2$O), 8.12 (d, *J* = 8.6 Hz, 2H, AB-system), 7.88 (d, *J* = 8.6 Hz, 2H, AB-system), 7.82 (s, 1H, resorcinol-H), 7.80–7.75 (m, 3H, phenyl group), 7.75–7.66 (m, 1H, phenyl group), 7.63–7.56 (m, 2H, phenyl group), 7.52 (d, *J* = 8.5 Hz, 2H, AB-system), 7.18 (d, *J* = 8.5 Hz, 2H, AB-system), 7.14 (s, 2H, NH$_2$, exchangeable by D$_2$O), 6.83 (d, *J* = 9.0 Hz, 1H, resorcinol-H), 4.80 (s, 1H, pyrane-H). ^{13}C NMR (101 MHz, DMSO-d_6, δ ppm): 195.61, 159.94, 154.42, 153.39, 153.28, 144.85, 138.80, 137.28, 135.69, 133.40, 131.87, 131.34, 130.10, 129.99, 129.15, 124.82, 122.97, 120.45, 120.21, 112.47, 109.27, 57.13, 36.55. MS (*m/z*): 550 (M$^+$, 30.14%). Anal. calcd for C$_{29}$H$_{19}$BrN$_4$O$_3$ (550.06): C, 63.17; H, 3.47; N, 10.16; found: C, 63.06; H, 3.38; N, 10.02%.

2.1.4. (*E*)-2-Amino-6-((4-benzoylphenyl)diazenyl)-7-hydroxy-4-(4-methoxyphenyl)-4*H*-chromene-3-carbonitrile 6c. Orange colour solid (1,4-dioxane), yield 87%, m.p. 251–252 °C, FT-IR (KBr, ν_{max}/cm^{-1}); 3419, 3329, 3213 (OH/NH$_2$), 3074 (Arom-CH), 2974, 2843 (Aliph-CH), 2191 (CN), 1651 (C=O), and 1586 (N=N). ^{1}H NMR (400 MHz, DMSO-d_6, δ ppm): 12.15 (s, 1H, OH, exchangeable by D$_2$O), 8.12 (d, *J* = 8.6 Hz, 2H, AB-system), 7.89 (d, *J* = 8.6 Hz, 2H, AB-system), 7.81 (s, 1H, resorcinol-H), 7.79–7.76 (m, 2H, phenyl group), 7.75–7.67 (m, 1H, phenyl group), 7.59 (t, *J* = 7.6 Hz, 2H, phenyl group), 7.13 (d, *J* = 8.7 Hz, 2H, AB-system), 7.05 (s, 2H, NH$_2$, exchangeable by D$_2$O), 6.87 (d, *J* = 8.7 Hz, 2H, AB-system), 6.82 (d, *J* = 9.0 Hz, 1H, resorcinol-H), 4.73 (s, 1H, pyrane-H), 3.71 (s, 3H, OCH$_3$). ^{13}C NMR (101 MHz, DMSO-d_6, δ ppm): 195.59, 159.92, 158.49, 154.28, 153.39, 153.31, 138.77, 137.56, 137.29, 135.64, 133.39, 131.35, 130.10, 129.14, 128.73, 124.87, 122.94, 120.69, 114.33, 113.46, 109.23, 57.96, 55.53, 36.19. MS (*m/z*): 502 (M$^+$, 21.98%). Anal. calcd for C$_{30}$H$_{22}$N$_4$O$_4$ (502.16): C, 71.70; H, 4.41; N, 11.15; found: C, 71.59; H, 4.31; N, 11.03%.

2.1.5. (*E*)-2-Amino-6-((4-benzoylphenyl)diazenyl)-4-(4-ethoxyphenyl)-7-hydroxy-4*H*-chromene-3-carbonitrile 6d. Orange colour solid (1,4-dioxane), yield 85%, m.p. 220–221 °C, FT-IR (KBr, ν_{max}/cm^{-1}); 3300, 3251, 3191 (OH/NH$_2$), 3061 (Arom-CH), 2982, 2879 (Alip-CH), 2198 (CN), 1647 (C=O), and 1589 (N=N). ^{1}H NMR (300 MHz, DMSO-d_6, δ ppm): 12.18 (s, 1H, OH, exchangeable by D$_2$O), 8.09 (d, *J* = 7.9 Hz, 2H, AB-system), 7.95 (d, *J* = 8.3 Hz, 1H, resorcinol-H), 7.87 (d, *J* = 7.9 Hz, 2H, AB-system), 7.82–7.64 (m, 3H, phenyl group), 7.57 (t, *J* = 7.2 Hz, 2H, phenyl group), 7.10 (d, *J* = 8.0 Hz, 2H, AB-system), 7.01 (s, 2H, NH$_2$, exchangeable by D$_2$O), 6.84 (d, *J* = 9.0 Hz, 2H, AB-system),

6.79 (s, 1H, resorcinol-H), 4.71 (s, 1H, pyrane-H), 3.96 (q, J = 6.7 Hz, 2H, OCH$_2$), 1.28 (t, J = 6.8 Hz, 3H, CH$_3$). ^{13}C NMR (101 MHz, DMSO-d_6, δ ppm): 195.04, 160.39, 159.46, 157.31, 153.79, 152.84, 138.26, 136.84, 135.11, 133.42, 132.87, 130.87, 129.62, 128.64, 128.26, 124.69, 122.42, 120.23, 115.51, 114.30, 108.75, 62.97, 57.55, 35.74, 14.67. MS (m/z): 516 (M$^+$, 7.79%). Anal. calcd for C$_{31}$H$_{24}$N$_4$O$_4$ (516.18): C, 72.08; H, 4.68; N, 10.85; found: C, 71.97; H, 4.59; N, 10.73%.

2.2. Dyeing and preparing dye dispersions

Polyester was dyed using AHIBA's infrared dyeing equipment in laboratory. The dye bath (20 mL) also contained 2.0 mL L^{-1} of Kimi-levelling ES, a fatty acid ester-based leveling and dispersing agent supplied by an Egyptian chemical company.[50] The previously mentioned disperse dye was prepared. Glacial acetic acid was employed to adjust the dye bath pH to 2, 4, and 6, whereas sodium hydroxide was used to increase it to 10.[50] The polyester textiles were immersed in the dye bath, which was gradually heated at a rate of 2 °C per minute. The temperature was raised gradually to the range of 100–130 °C. This high temperature is kept in the dye bath for 15, 30, 45, or 60 minutes depending on the desired temperature.[51,52] An aqueous solution of 2 g L^{-1} sodium hydroxide and 2 g L^{-1} sodium hydrosulfite with a liquor ratio of 1:20 was utilized for the reduction clearing operation, which was carried out at 85 °C for 20 minutes.[53,54]

2.3. Biological activity of dyed-fabric samples

To test the dyed-fabric samples for their possible repellency properties against the blood sucking animal model, *Culex pipiens* mosquitoes of well-known public health significance were selected to investigate this possibility.

2.3.1. Mosquito colony. Laboratory-strain *Culex pipiens* larvae were obtained from an established colony maintained at the Medical Entomology Insectary, Al-Azhar University, Cairo, Egypt. The larvae were maintained under controlled laboratory conditions (27 ± 2 °C, 75 ± 5% relative humidity, with a 14-h light/10-h dark photoperiod) until reaching adulthood. Adult mosquitoes were provided with a 10% sucrose solution, while females were offered pigeon blood to facilitate reproduction. Subsequently, the laid eggs were carefully moved to plastic cups containing 500 mL of distilled water, where they hatched for experimental use.[55]

2.3.2. Biochemical assay. First-instar larvae from the colony were treated in triplicate with the tested materials, namely **6a**, **6b**, **6c**, and **6d** solubilized in dimethyl sulfoxide (DMSO), along with an untreated control group. We monitored molting and exuviae, and once larvae reached the third instar, we collected fifty larvae from each treatment, which were then homogenized in distilled water using a Teflon homogenizer on crushed ice for 5 minutes. The homogenized specimens were centrifuged at 6000 rpm for 10 minutes in a refrigerated centrifuge, and the resulting supernatant was collected for biochemical assays. Acetylcholinesterase (AChE) activity was measured using acetylcholine bromide as a substrate,[56] while GST activity was determined using 1-chloro-2,4-dinitrobenzene as a substrate.[57]

2.3.3. Repellency properties of dyed-fabric samples. We evaluated the mosquito repellency of dyed fabric samples, namely **6a**, **6b**, **6c**, and **6d**, against 72-hour starved female mosquitoes collected from the established colony. Glass cubes (200 cm^3 (5 × 5 × 8 cm^3)) were covered with fabric samples stained with the tested materials. Pigeons, with abdominal feathers removed, were then placed on the fabric-covered cubes for 2 hours. A 15% DEET solution (Johnson Wax, Egypt) applied to a clean fabric sample served as the positive control, whereas DMSO was used as the negative control. All treatments were performed in triplicate in separate cages. The numbers of fed and unfed females were recorded and calculated at 30-minute intervals.[58]

2.3.4. Statistical analysis. For each treatment, descriptive statistics, including the mean and standard error (SE), were computed using SPSS (IBM SPSS, version 25). Repellency (%) was calculated using the formula: $(A\% - B\%/100 - B\%) \times 100$, where A is the percentage of unfed females in the treatment and B is the percentage of unfed females in the negative control.[58]

2.3.5. Molecular docking. The structures of the compounds were generated in the PDB file format from the outputs of Gaussian 09. The crystal structures of AChE (PDB ID: 5x61) and GST (PDB ID: 1PN9) were retrieved from the Protein Data Bank (https://www.rcsb.org/pdb). Molecular docking studies were carried out using MOE 2015 software.

3. Results and discussion

3.1. Organic synthesis

The therapeutic potential of the target molecules was enhanced once the heterocyclic component was integrated into the azo dye framework. Drugs can be easily adjusted for an assortment of biological and pharmacological purposes by including a heterocyclic moiety. The procedure adopted in this study for the synthesis of the desired 4*H*-chromene substituted azo benzophenones **6a–d** is depicted in Scheme 2. As outlined in Scheme 1, the requisite compound **4** was first synthesized by
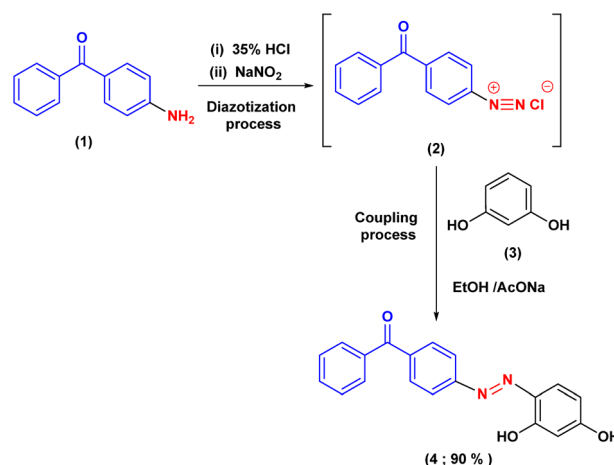
Scheme 1 The synthetic methodology utilized for the synthesis of azo dye **4**.
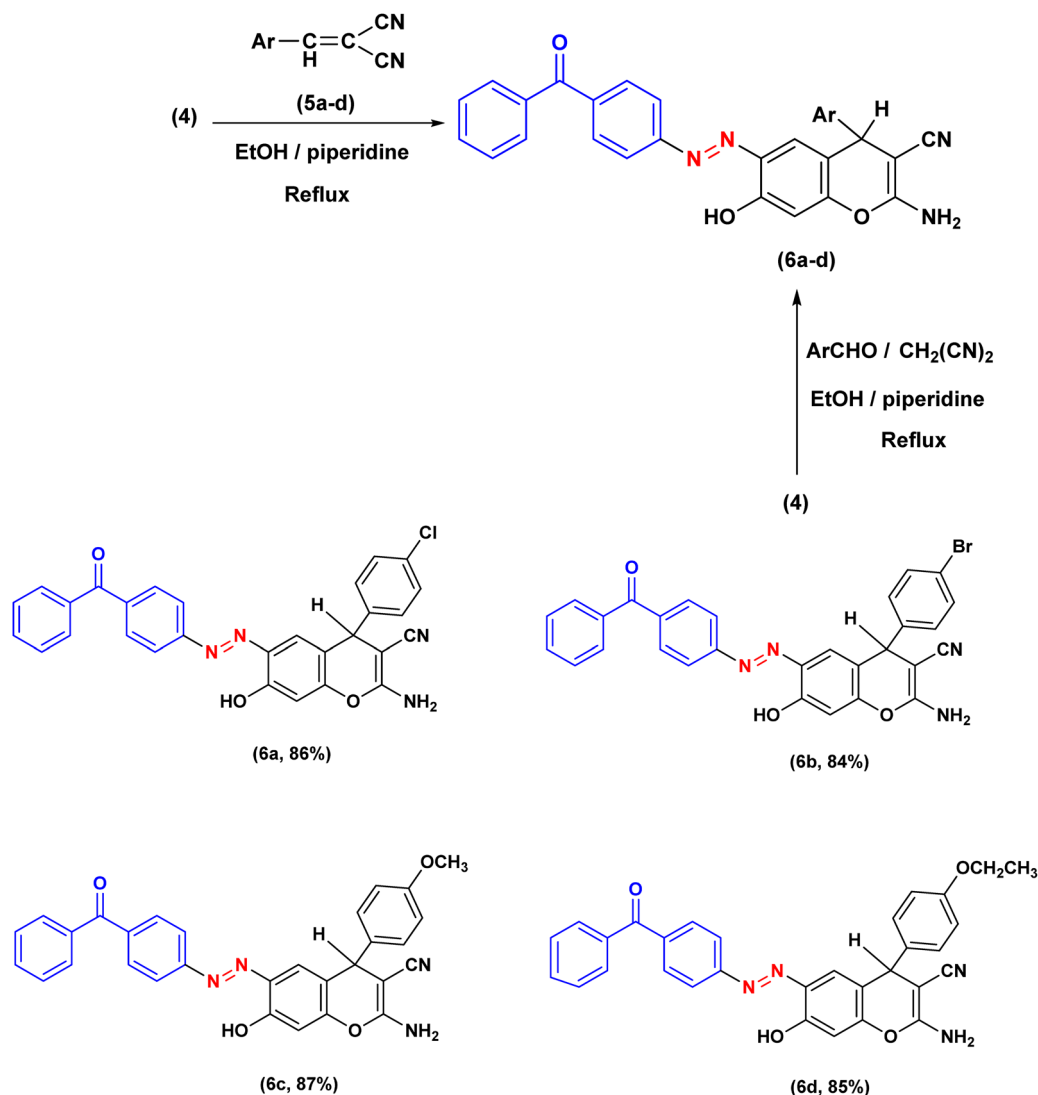
Scheme 2 The synthetic approach employed for the preparation of 2-amino-4*H*-chromene-3-carbonitriles.

diazotising 4-aminobenzophenone **1** and then coupling with resorcinol **3**.[59]

The 2-amino-4*H*-chromene-3-carbonitriles **6a–d** were efficiently synthesized *via* a one-pot reaction of compound **4** with arylidene-malononitriles **5** in ethanol using piperidine as a catalyst under reflux conditions. High yields were achieved for all the created molecules, falling within the range of 84–87%. The chemical structures of the isolated chromenes were demonstrated through extensive spectroscopic investigations. Elemental evaluation provided results consistent with the theoretical percentages, indicating the high purity of the obtained products. The infrared spectra of the isolated products indicated distinctive absorption bands corresponding to amino, cyano, carbonyl, and azo functional groups. The infrared spectrum of compound **6a**, utilized as an illustrative model, displayed prominent absorption bands corresponding to the OH, NH$_2$, CN, and N=N functional groups at 3300, 3251, 3191, 2198, 1647, and 1589 cm^{-1}, respectively. The proton nuclear

magnetic resonance spectrum of molecule **6d** presented a singlet at δ_H 4.71 ppm, which is attributed to the methine proton of the chromene ring. Additionally, two downfield signals were observed at δ_H 12.18 and 7.01 ppm, which are exchangeable with D$_2$O and correspond to the hydroxyl and NH$_2$ protons, respectively. Two doublets at δ_H 7.87 (J = 7.9 Hz) and 8.09 (J = 6.8 Hz) ppm were designated to an AB system, while a triplet at δ_H 1.28 ppm (J = 6.8 Hz) and a quartet at δ_H 3.96 ppm (J = 6.7 Hz) were observed and attributed to the ethyl group. Furthermore, the remaining aromatic protons were observed as a doublet at δ_H 7.95 (J = 8.3 Hz) and a singlet at δ_H 6.79 ppm, corresponding to the resorcinol protons; two doublets at δ_H 6.84 (J = 9.0 Hz) and 7.10 (J = 8.0 Hz) ppm, a triplet at δ_H 7.57 ppm (J = 7.2 Hz), as well as a multiplet at δ_H 7.82–7.64 ppm were also identified. In the carbon nuclear magnetic resonance spectrum of **6d**, the downfield resonance at δ_C 195.04 ppm was assigned to the carbonyl moiety, whereas the signal at δ_C 115.51 ppm was attributed to the nitrile carbon
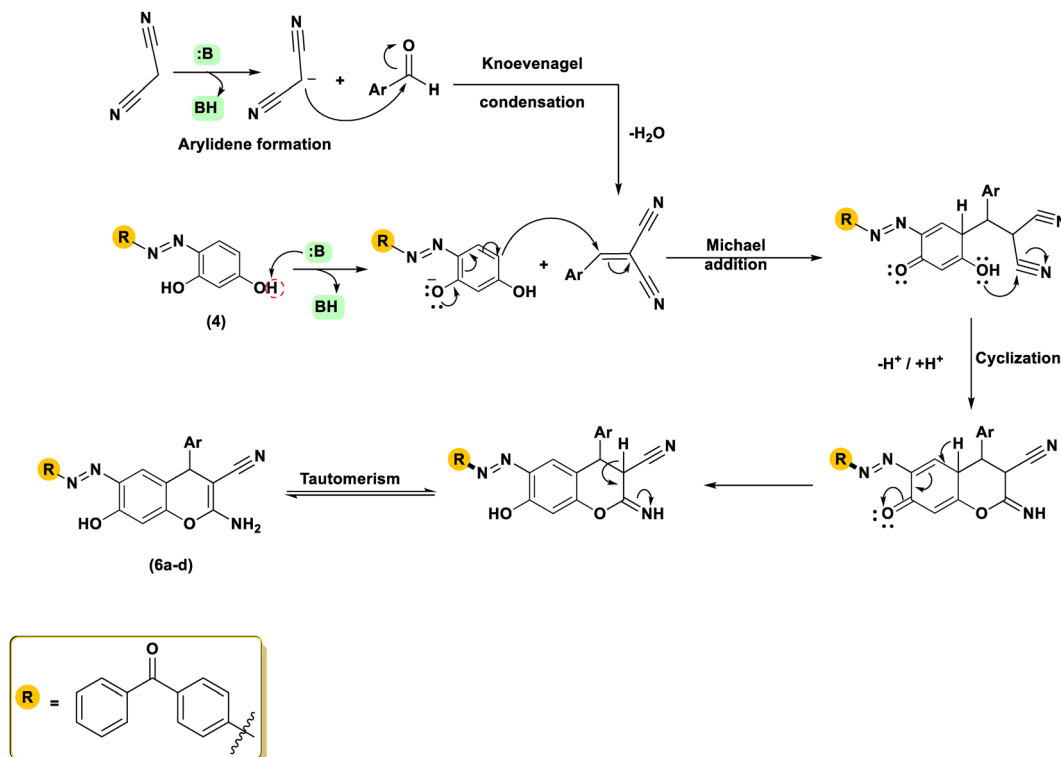
Scheme 3 Feasible mechanistic pathway for the generation of 2-amino-4H-chromenes **6a–d**.

at position C-3. Furthermore, the singlet at δ_C 62.97 ppm was attributed to the methylene carbon, while the terminal carbon of the ethoxy group appeared at δ_C 14.67 ppm. The peak at 35.74 ppm in the spectrum is attributed to the benzylic C-4 carbon located within the pyran ring. The ^{13}C NMR spectrum also displayed signals at δ_C = 160.39, 159.46, 157.31, 153.79, 152.84, 138.26, 136.84, 135.11, 133.42, 132.87, 130.87, 129.62, 128.64, 128.64, 128.64, 128.64, 128.26, 124.69, 122.42, 120.23, 114.30, 108.75, and 57.55 (C_3), representing the several kinds of carbon atoms that make up the molecule. The mass spectroscopy of compound **6c** revealed a noticeable molecular ion at

m/z 502 (21.98%), which is in agreement with the proposed molecular formula $C_{30}H_{22}N_4O_4$. The achievable multi-step mechanism for the synthesis of 4H-chromene-3-carbonitriles **6** under organo-base conditions is proposed and illustrated in Scheme 3. The mechanism of this reaction involves sequential steps, including a Knoevenagel condensation, a Michael addition, and an intramolecular cyclization, which collectively lead to the formation of the final product.[21] The development of 4H-chromene **6** is assumed through the deprotonation of resorcinol **4** to generate the reactive intermediate **A**, subsequently followed by Michael addition to the double bond in **5**.
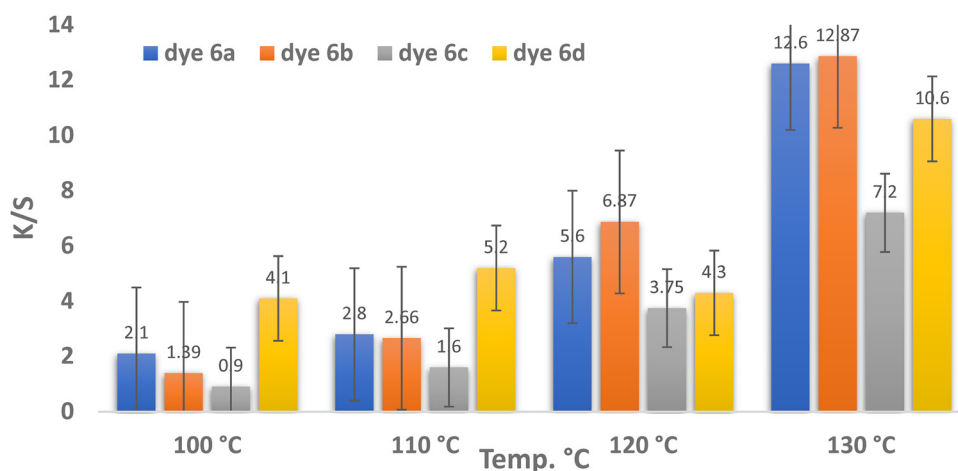
Fig. 2 Temperature and color strength (K/S) relationship for dyes **6a–d** (pH = 4, time = 30 min, and 3% shade).

The Michael adduct **B** subsequently underwent efficient cyclisation through intramolecular attack of the oxygen atom on the cyano carbon, affording the heterocyclisation products **6a–d**. Further confirmation of the structure of 2-amino-4*H*-chromenes **6** was obtained *via* independent synthesis using a one-pot, ternary reaction of resorcinol **4**, an aromatic aldehyde, and malononitrile (1:1:1 molar ratio) with a catalytic amount of piperidine at reflux temperature in ethanol melting point (m.p), Thin Layer Chromatography (TLC) and IR (Infrared) spectrum.

3.2. ClogP computation

The ClogP values, representing the *N*-octanol/water partition coefficients of the synthesized dyes, were calculated using Chem-Draw. The effectiveness of polyester dyeing depends on how disperse dyes are distributed between the polyester fibers

Table 1 Measurements of L^*, a^*, b^*, E, H°, C^*, color strength (K/S) and reflectance ($R\%$) affected by the dyeing temperatures of dyes **6a–d** (pH = 4, time = 30 min, and 3% shade)

Dye	Temp. (°C)	L^*	a^*	b^*	C^*	H°	CMC ΔE	K/S	$R\%$	Color shades of dyeing fiber
6a	100	73.6	16.3	29.5	33.7	61.1	—	2.1	18.91	
	110	73	18.3	34.4	39	62	2.56	2.8	14.94	
	120	65.6	24.5	40.3	47.2	56.7	7.28	5.6	7.67	
	130	58.8	33.6	47.8	58.4	54.9	14.1	12.6	3.67	
6b	100	77.2	14.6	29.1	32.6	63.4	—	1.39	21.84	
	110	70	21.7	33.3	39.7	56.9	6.19	2.66	13.93	
	120	64.2	31.2	43.3	53.4	54.2	13.44	6.87	6.38	
	130	58.4	38.3	49.3	62.4	52.1	18.82	12.87	3.61	
6c	100	84.1	2.4	25	25.2	84.5	—	0.9	29.3	
	110	80	8.8	35.2	36.3	75.9	7.6	1.6	19.32	
	120	76.2	14.2	45.5	47.7	72.7	14.33	3.75	10.58	
	130	71	21	51	55.2	67.7	19.99	7.2	6.09	
6d	100	81	10.6	48.6	49.7	77.7	—	4.1	12.01	
	110	75.2	15.8	50.3	52.7	72.6	4.19	5.2	9.34	
	120	76.3	13.1	50.9	52.5	75.6	2.49	4.3	9.6	
	130	67.2	25.8	58.2	63.6	66.1	11.35	10.6	4.34	

Table 2 easurements of color, color strength (K/S) and reflectance ($R\%$) affected by the dyeing pH of dyes **6a–d** (temperature = 130 °C, time = 30 min, and 3% shade)

Dye	pH	L^*	a^*	b^*	C^*	$H°$	E	K/S	$R\%$	Color shades of dyeing fiber
	2	57.5	33.7	46.4	57.4	54.1	—	12.5	3.68	
	4	63.4	28.4	49.1	56.7	60	6.39	9.8	4.67	
6a	6	66	19.9	49.2	53.1	68	14	8	5.6	
	8	65.7	20.3	49.5	53.5	67.7	13.7	8.2	5.5	
	10	67.7	18.4	50.2	53.4	69.9	15.9	7.6	5.79	
	2	61.5	34.1	50.4	60.9	56	—	11.6	4.01	
	4	64.8	29.4	63	60.6	61	5.4	10.4	4.38	
6b	6	64	23.7	47.1	52.7	63.3	7.75	7.9	5.61	
	8	61.8	27.8	48.4	55.8	60.1	4.48	9.3	4.9	
	10	65.7	23.1	51	56	65.7	9.9	8.8	5.1	
	2	65.2	30.3	54.6	62.5	61	—	11.8	4.25	
	4	68.8	25.4	53	58.7	64.4	3.75	8.1	5.49	
6c	6	68.7	20.9	51.6	55.7	67.9	6.88	7	6.28	
	8	73.4	20.8	59.4	62.9	70.7	9.91	6.8	6.38	
	10	74.7	16.6	57	59.3	73.8	12.6	6	7.2	
	2	68.7	25.3	57.1	62.5	66.1	—	9.7	4.86	
	4	64.5	28.7	58.6	65.2	63.9	2.77	12.6	3.69	
6d	6	66.1	24.8	58.5	63.6	67	1.35	11	4.16	
	8	69.5	27.3	66.7	72.1	67.8	3.76	11.8	3.89	
	10	71.5	24.4	67.4	71.7	70.1	5.07	11.3	4.09	

and the surrounding water. Consequently, dyes exhibiting lower solubility in the aqueous dye bath (*i.e.*, higher hydrophobicity) tend to penetrate more efficiently into the hydrophobic polyester matrix. Thus, the relevance of ClogP values is discussed in the following section. Generally, dyes with lower ClogP values are more soluble in the aqueous dye bath, which tends to result in lower *K*/*S* values.[60] Consistent with this relationship, dyes **6d** and **6c**, which exhibit the lowest ClogP values (7.62446 and 7.09546, respectively), demonstrated the highest solubility. Conversely, dyes **6b** and **6a**, with higher ClogP values (8.03946 and 7.88946, respectively), are expected to yield higher *K*/*S* ratios due to their reduced aqueous solubility. These findings confirm that the ClogP values are in good agreement with the observed *K*/*S* values.

3.3. Characteristics of dyeing polyester fabrics

3.3.1. Depth of shade. Polyester fabrics were dyed in the presence of dispersing leveling agents at 100 to 130 °C for 15 to 60 minutes, under pH conditions between 2 and 10, and at

varying shade levels of 1–5%. A variety of color tones, including yellowish brown, beige, reddish brown, reddish yellow, and brown, were produced by dyeing the polyester materials. In polyester dyeing, the depth of shade is closely proportional to certain dyeing variables, mainly temperature, time, and dye concentration, which affect the amount of dispersed dye that is absorbed and fixed inside the fiber.[59,65]

3.3.2. Analysis and measurements of color strength (*K*/*S*). The dyeing performance of dyes on textile surfaces is often described using *K*/*S* values at wavelengths that correspond to minimum reflectance and maximum absorbance (400, 380, 390, and 400 nm) for dyes **6a–d**, respectively. It was observed that, for all dyed fabrics **6a–d**, the a^* and b^* values were positive, and these values demonstrate how the color hues of the dye have shifted, becoming more reddish on the red-green axis and more yellowish on the yellow-blue axis. Positive hue angle (H°) values for all synthetic dyes **6a–d** indicate a shift toward a yellowish hue, whereas negative H° values correspond to a shift toward a reddish hue. A fabric's reflectance value indicates how much visible light it reflects, while the *K*/*S* values
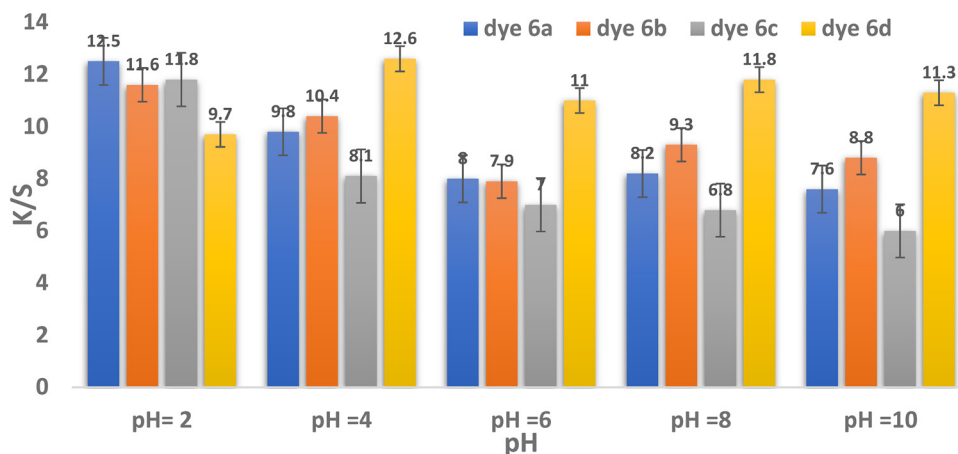

Fig. 3 pH and color strength (*K*/*S*) relationship for dyes **6a–d** (temperature = 130 °C, time = 30 min, and 3% shade).
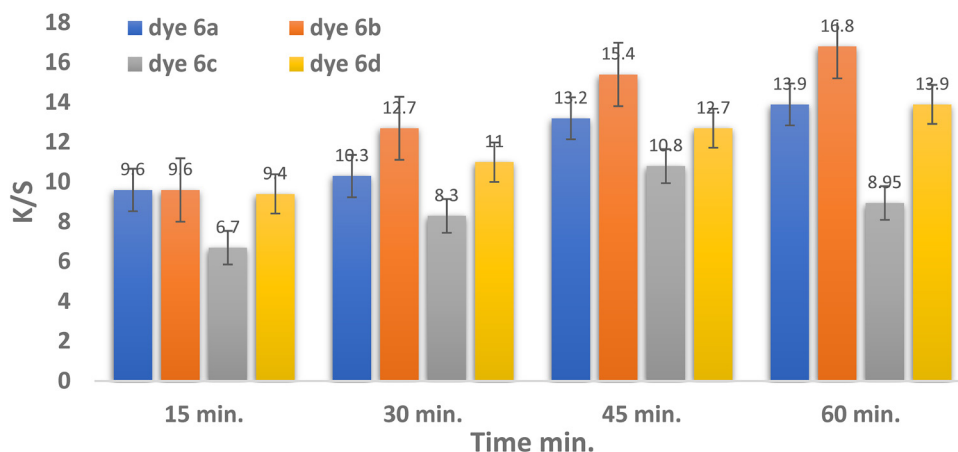

Fig. 4 Time and color strength (*K*/*S*) relationship for dyes **6a–d** (temperature = 130 °C, pH = 2 for dyes **6a–c** and pH = 4 in the case of dye **6d**, and 3% shade).

depend on the chemical structure and substituents of the aromatic moiety, producing varying dyeing strengths.[61]

3.3.3. Dyeing temperature's effect on reflectance (R%) and color strength (K/S).

In this technique, polyester materials were dyed using four disperse dyes at temperatures ranging from 100 to 130 °C. Because disperse dyes require temperatures above their glass transition point (80 °C) to dye polyester effectively, this study began at 100 °C, following the common practice in earlier studies. Fig. 2 and Table 1 present the effect of temperature variations on the color strength (K/S) values of polyester fabrics compared to standard dyeing at 100 °C.[54,62] As the dye bath temperature increases, the K/S values of polyester fabrics also increase, as illustrated in Fig. 2.

Fig. 2 shows that the optimum dyeing temperature for dyes **6a–d** was 130 °C, corresponding to K/S values of 12.6, 12.87, 7.2, and 10.6, respectively. This implies that the restriction temperature of 130 °C is ideal for dispersing all dyes. These phenomena can be attributed to the high kinetic energy of the dye molecules and their rapid dispersion rates. The highest K/S values for dyes **6a** and **6b** were observed at 130 °C, recording 12.6 and 12.87, respectively. This behavior may be attributed to their chemical structures, which incorporate chlorine and

Table 3 Measurements of color, color strength (K/S) and reflectance (R%) affected by the dyeing durations of dyes **6a–d** (temperature = 130 °C, pH = 2 for dyes **6a–c** and pH = 4 in the case of dye **6d**, and 3% shade)

Dye	Time (min)	L*	a*	b*	c*	H°	CMC ΔE	K/S	R%	Color shades
6a	15	61.1	29.4	45.5	54.2	57.1	—	9.6	4.72	
	30	61.5	30.6	46.6	55.8	56.7	0.75	10.3	4.44	
	45	58.2	34.8	47.8	59.1	53.9	4.05	13.2	3.6	
	60	57.6	35.3	48.6	60.1	54	3.88	13.9	3.36	
6b	15	62.8	30.5	48	56.9	57.6	—	9.6	4.71	
	30	58.4	36.3	48.4	60.5	53.1	4.95	12.7	3.68	
	45	55.8	41.9	49.1	64.5	49.5	9.21	15.4	3.06	
	60	54.1	41.5	49	64.2	49.7	9.24	16.8	2.83	
6c	15	74.4	18.2	55.4	58.3	71.8	—	6.7	6.5	
	30	71.7	22	55.5	59.7	68.4	2.92	8.3	5.44	
	45	68.6	26	57.6	63.2	65.7	5.71	10.8	4.24	
	60	71.8	19.9	56.5	59.9	70.6	1.5	8.95	5.03	
6d	15	70.7	26.9	61	66.7	66.2	—	9.4	4.82	
	30	67.9	27.2	60.1	66	65.7	1.24	11	4.19	
	45	66.5	28.1	61.4	67.5	65.4	1.84	12.7	3.69	
	60	64.8	30.5	61.8	68.9	63.7	3.36	13.9	3.35	

Table 4 Measurements of color, color strength (K/S) and reflectance ($R\%$) affected by the dyeing shades of dyes **6a–d** (temperature = 130 °C, pH = 2 for dyes **6a–c** and pH = 4 in the case of dye **6d**, and duration = 60 min for dyes **6a, b, and d and** duration = 45 min for dye **6c**)

Dye	Shade%	L^*	a^*	b^*	C^*	$H°$	E	K/S	$R\%$	Color shades of dyeing fiber
	1%	57.7	33.6	46.5	57.4	54.2	—	12.8	3.64	
	2%	60.1	36.8	51.2	63.1	54.3	0.04	13.5	3.43	
6a	3%	60	36.9	51.2	63.1	54.2	2.24	13.6	3.38	
	4%	52.8	39.6	46.5	61.1	49.6	5.75	16.7	2.91	
	5%	50.3	41.6	48.5	63.9	50.9	6.3	18.2	2.6	
	1%	62.5	32.6	51.1	60.6	57.5	4.52	10.5	4.14	
	2%	58	39.8	51.5	65.1	52.3	1.56	14.2	3.27	
6b	3%	59.6	39.1	53.1	65.9	53.6	—	14.4	3.16	
	4%	53.5	41.1	48.5	63.6	49.7	4.92	17	2.81	
	5%	52.3	43.8	48.2	65.1	47.7	7.03	17.4	2.69	
	1%	71	22.1	55.7	60	68.3	11.1	8.4	5.33	
	2%	65.2	33.4	52.4	62.1	57.5	—	10.5	4.34	
6c	3%	68.6	30.1	60.1	67.2	63.4	6.65	12.2	3.81	
	4%	69.3	29.4	62.6	69.2	64.8	8.43	13.4	3.46	
	5%	66.1	33.2	63.1	71.4	62.2	6.12	15.4	3.05	
	1%	71	22.1	55.7	60	68.3	11.1	8.4	5.33	
6d	2%	70.4	26.6	60.2	65.8	66.2	3.13	9.5	4.78	

Table 4 (continued)

Dye	Shade%	L^*	a^*	b^*	C^*	$H°$	E	K/S	$R\%$	Color shades of dyeing fiber
	3%	65.3	31.8	56.5	64.9	60.7	5.86	11.6	4	
	4%	63.3	34	63.5	72	61.8	7.28	15.9	2.96	
	5%	59.5	37.3	61.7	72.1	58.8	9.68	19.2	2.59	
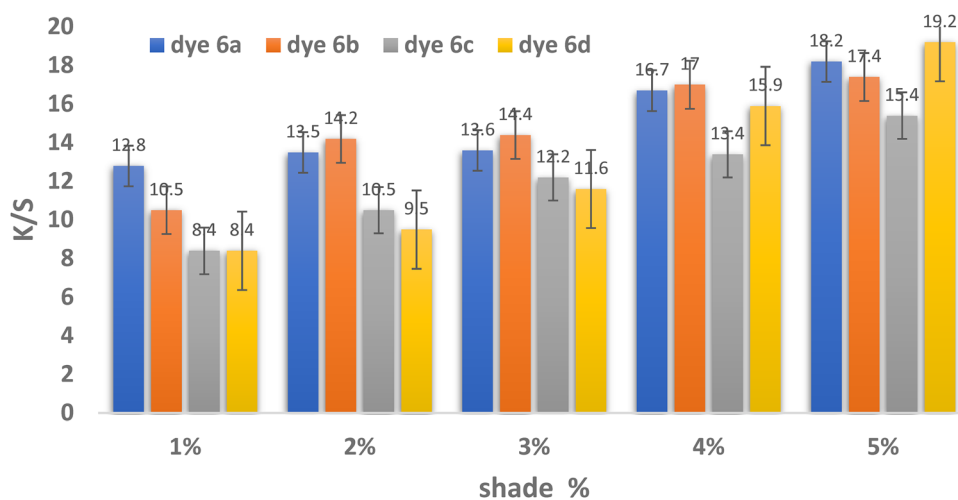
Fig. 5 Shade and color strength (K/S) relationship for dyes **6a–d** (temperature = 130 °C, pH = 2 for dyes **6a–c** and pH = 4 in the case of dye **6d**, and duration = 60 min for dyes **6a, b, and d** and duration = 45 min for dye **6c**).
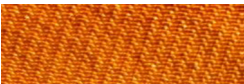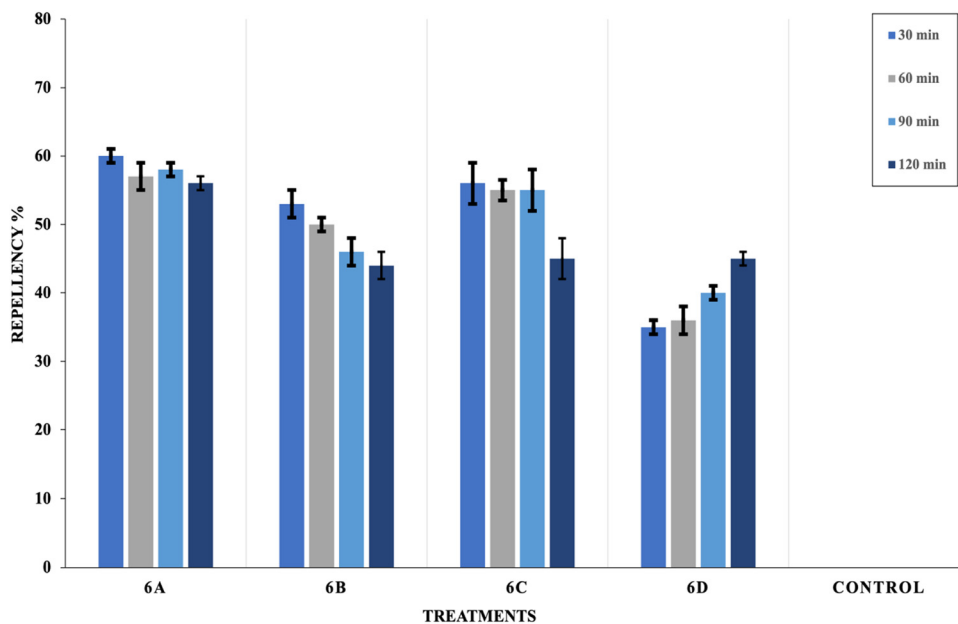

Fig. 6 Repellent effect of the tested materials for two consecutive hours against adult female *Culex pipiens* mosquitoes.
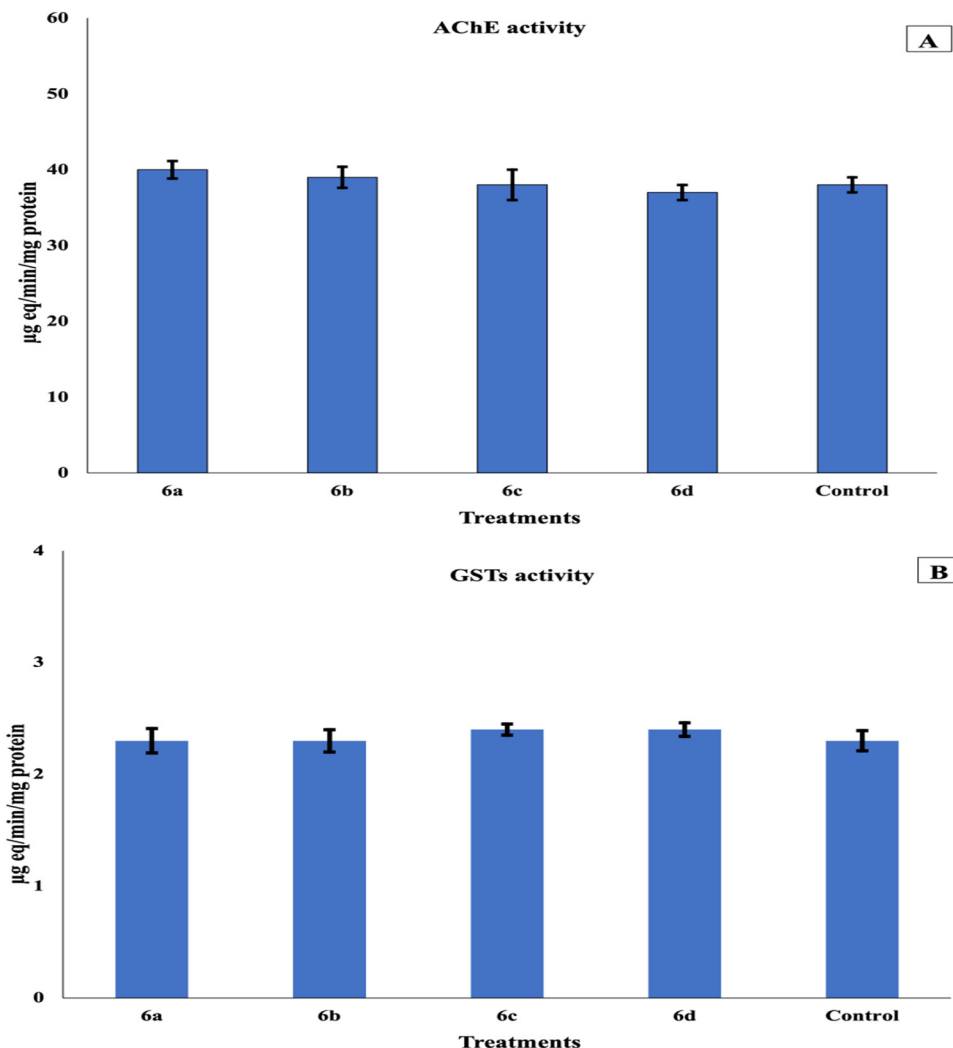
Fig. 7 Effect of tested materials on the enzymatic activities of acetylcholinesterase (AChE) (A) and glutathione S-transferase (GST) (B) in the third larval instar of the mosquito *Culex pipiens*. Bars with different letters are significantly different ($p < 0.05$). Data are presented as mean ± SE of three replicates.

Table 5 Docking interaction data calculations of the co-crystallized control ligand (EPE) in the enzyme binding pocket and **6a**, **6d**, **6c**, and **6b** molecules with the active site of the AChE receptor (PDB ID: 5x61)

Molecule	Ligand	Receptor	Interaction	Distance (in Å from the main residue)	E (kcal mol^{-1})	S (kcal mol^{-1})
6a	N54	GLU 359	H-donor	3.03	−2	−8.4233
	N15	GLY 601	H-acceptor	3.41	−1.2	
6d	N15	TYR 291	H-acceptor	3.02	−1.9	−7.8642
	6-Ring	TRP 245	pi–pi	3.75	0	
	6-Ring	TRP 245	pi–pi	3.99	0	
	6-Ring	TYR 493	pi–pi	3.81	0	
6c	O31	ILE 231	H-donor	3.39	−0.7	−7.7104
	6-Ring	TRP 245	pi–pi	3.54	0	
6b	N54	GLU 359	H-donor	2.96	−4.6	−7.427
	6-Ring	TYR 494	pi–H	4.17	−0.6	
EPE (control ligand)	O32	ASN 246	H-donor	2.62	−0.6	−5.3571
	O23	SER 360	H-acceptor	2.77	−1.8	
	O32	ASP 233	H-acceptor	2.92	−2.8	

bromine substituents that enhance the electron-accepting ability, thereby promoting stronger interactions with polyester fibers.[63] As

the temperature increases for all dyes, the reflectance values decrease, as shown in Table 1 and Fig. 2.
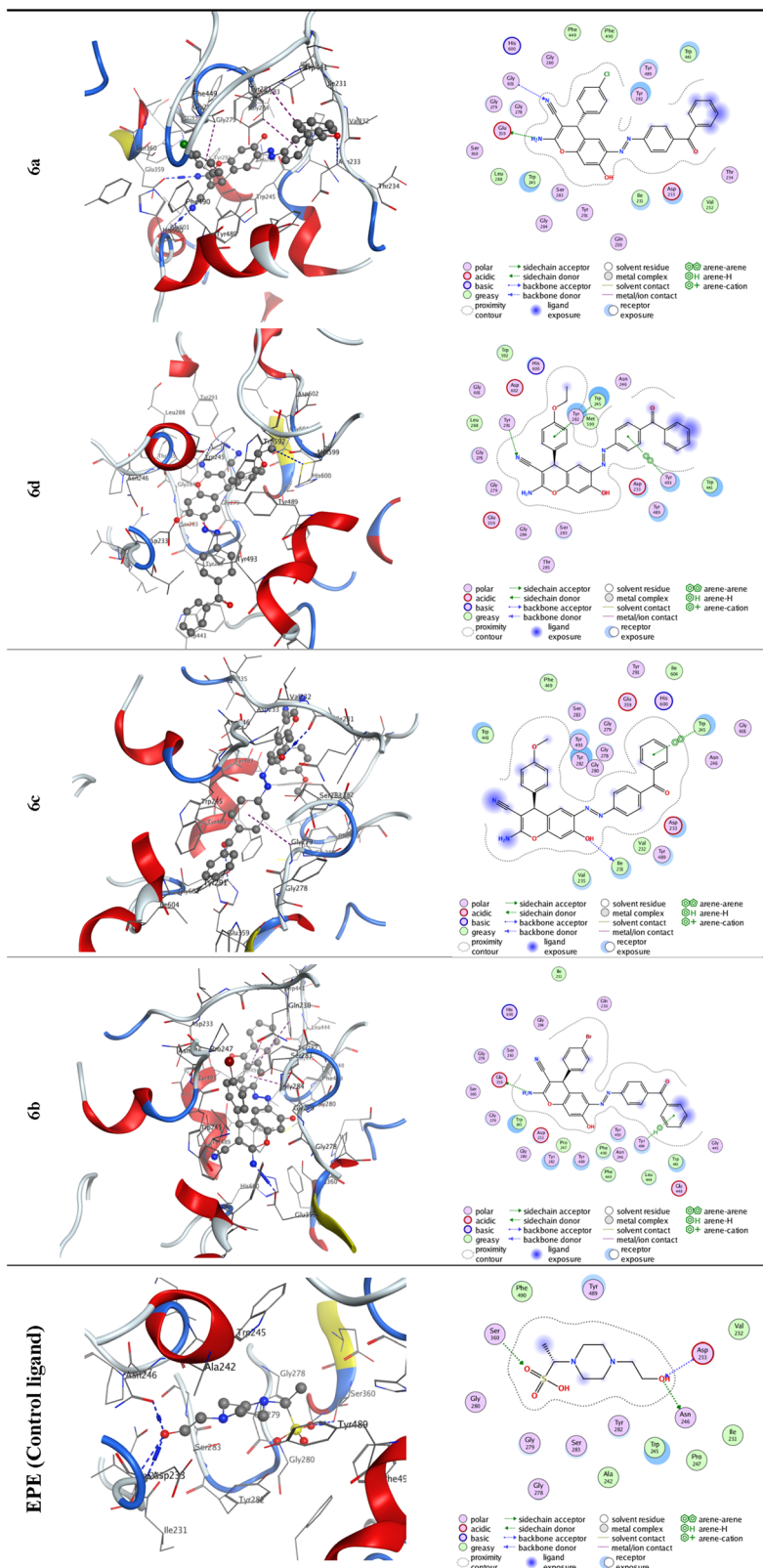
Fig. 8 2D and 3D molecular docking simulation studies of the interactions between the co-crystallized control ligand (EPE) in the enzyme binding pocket and **6a**, **6d**, **6c**, and **6b** molecules with the active site of the AChE receptor (PDB ID: 5x61).

3.3.4. Effect of dyeing pH on color strength (K/S) and reflectance ($R\%$). Table 2 and Fig. 3 illustrate the variations in the K/S values of dyes **6a–d** at pH values of 2, 4, 6, 8, and 10. This also suggests that the dyeing behavior of the colors is strongly influenced by pH variations during the process of dyeing. As shown in Table 2 and Fig. 3, dye **6d** exhibited the highest K/S value at pH 4, whereas dyes **6a–c** showed lower reflectance and higher K/S values at pH 2. It is noteworthy that for dyes **6a–c**, pH 2 was more favorable than pH 4. In contrast, although the optimum pH for dye **6d** was 4, it exhibited a substantially higher color strength value (12.6) compared to dye **6c** (11.8), which may be attributed to its higher molecular weight.

However, polyester dyeing is commonly carried out under acidic pH conditions. As shown in Fig. 3 and Table 2, the findings indicate that the optimum pH for dyeing polyester with dyes **6a–c** is 2, whereas for dye **6d** it is 4.

3.3.5. Impact of dyeing time on color strength (K/S) and reflectance ($R\%$). Fig. 4 presents the K/S values of polyester fabrics dyed for different dyeing times (15, 30, 45, and 60 minutes). Polyester dyeing was performed at 130 °C for varying durations under acidic conditions, with pH 2 for dyes **6a–c** and pH 4 for dye **6d**. The color strength (K/S) increases with longer dyeing times until the dyeing equilibrium is reached.[64] As shown in Fig. 4 and Table 3, dyes **6a**, **6b**, and **6d** achieved their highest K/S values (13.9, 16.8, and 13.9, respectively) at 60 minutes of dyeing. After 60 minutes, the distribution of dye molecules between the fiber and the dye solution reached equilibrium. The demand for balance in the therapy bath and the potential for stripping from prolonged heating could account for this.[65] As shown in Table 3, the reflectance of all dyes gradually decreased with time and eventually became negligible.[66] The results of this investigation show that dyeing polyester in four colors for 60 minutes is the best duration, except for dye **6c**, for which the best duration is 45 minutes.

3.3.6. Impact of shade dyeing on color strength and reflectance. The color strength and reflectance values of polyester fabrics dyed with disperse dyes **6a–d** are shown in Table 4 and Fig. 5. Higher K/S values, reflecting greater color strength, were obtained when polyester was dyed at shade concentrations of 1, 2, 3, 4, and 5% of the original fabric weight. For dyes **6a** and **b**, the increase in K/S values from shade concentrations of 4% to 5% was negligible (1.5 and 0.4, respectively), as shown in

Table 4 and Fig. 5. This may be attributed to the saturation of dye particles within the pores of the polyester fibers, which prevents further absorption. At a 5% o.w.f. shade, the highest color intensity (K/S) values for disperse dyes **6a–d** were 18.2, 17.4, 15.4, and 19.2, respectively, as presented in Table 4 and Fig. 5. These results were obtained under the following conditions: pH 2 for dyes **6a–c** and pH 4 for dye **6d** at a dyeing temperature of 130 °C and a dyeing time of 30 minutes. This effect may be attributed to the saturation of dye particles within the pores of the polyester fibers, which hinders further absorption. For disperse dyes **6a–d**, the greatest color intensity values at 5% o.w.f. shade were 18.2, 17.4, 15.4, and 19.2, in that order.[67–69]

3.4. Repellency assessment of the dyed fabrics

Mosquitoes can travel up to 200 miles from their birthplace.[70] Consequently, numerous researchers, industries, and medical organizations are investigating mosquito repellents, which are finishing agents or treatments applied to skin, clothing, and other surfaces to deter mosquitoes. One of the sectors of the global textile industry that is expanding the fastest right now is smart or functional textiles. These smart technology applications also include protective textiles.[71] The purpose of protective textiles is to shield the wearer from insects, bacteria, fungi, heat, cold, and mosquitoes. Because medical textiles have a direct connection to people, they are also an area that needs a lot of attention.[72] Both the domestic and international markets for medical textiles have enormous potential. In addition to being classified as medical textiles, fabrics treated with natural materials to offer defense against bacteria and insect bites are becoming more and more significant to consumers.[73] Within this general framework, our research seeks to find natural alternatives. The results revealed that the repellent effect of **6a** reached about 60% after 30 minutes of treatment and continued for two hours until it became 56%. This time-dependent decline is likely attributable to volatilization because the active compound evaporates from the tissue substrate over time. Additionally, exposure to ambient light, particularly the UV spectrum, can induce chemical transformations, such as photolysis or photo-oxidation, of the active molecules.[74] The active compound may also slowly diffuse from the surface layer into the bulk structure of the fabric material; this reduces the surface concentration required for immediate

Table 6 Docking interaction data calculations of the co-crystallized control ligand (GTX) in the enzyme binding pocket and **6d**, **6a**, **6c**, and **6b** molecules with the active site of the receptor of GST (PDB ID: 1pn9)

| Molecule	Ligand	Receptor	Interaction	Distance (in Å from the main residue)	E (kcal mol^{-1})	S (kcal mol^{-1})
6d	N61	GLU 64	H-donor	3.01	−4.3	−6.6624
	N61	GLN 49	H-acceptor	3.23	5.9	
6a	N54	GLU 64	H-donor	3.36	−1.4	−6.2752
6c	O31	MET 34	H-donor	3.14	−3.2	−6.2494
	N15	SER 9	H-acceptor	3.38	−1.3	
	N15	ALA 10	H-acceptor	3.5	−1.5	
6b	O53	GLY 8	H-acceptor	3.34	−0.7	−6.0302
GTX (control ligand)	O11	SER 65	H-acceptor	3.27	−2.5	−5.7243
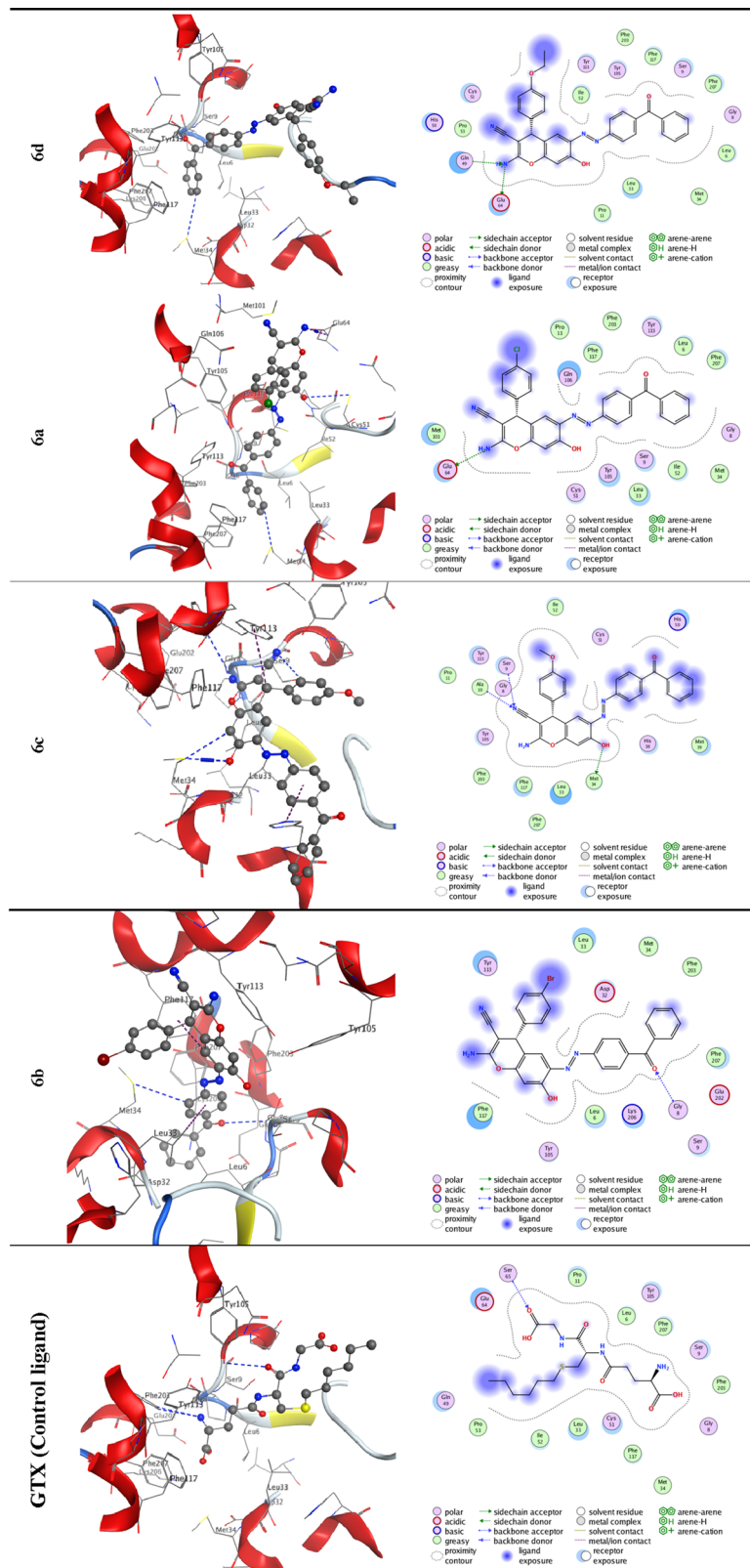
Fig. 9 2D and 3D molecular docking simulation studies of the interactions between the co-crystallized control ligand (EPE) in the enzyme binding pocket and **6a**, **6d**, **6c**, and **6b** molecules with the active site of the receptor of GST (PDB ID: 1pn9).

contact and vapor release.[69] The repellent effect percentages of compounds **6b**, **6c**, and **6d** became 53–44%, 56–45% and 35–

44%, respectively. In general, **6a** had the highest repellent effect, while **6d** had the least effect (Fig. 6). Our findings concur

with those of ref. 74, who found that textile materials, such as door curtains, military uniforms, bed linens, tablecloths, and sofa coverings, can be treated with insect repellent chemicals to provide external protection against mosquito bites. Consistent with our findings, three medical insect pests (*A. aegypti*, *A. albopictus*, and *Musca domestica*) were effectively knocked down and adulticidally controlled using essential oils (EOs) of *Cymbopogon citratus* and *Eucalyptus globulus*, as well as their mixtures.[75] Using the WHO cone test, several essential oils have been evaluated for their efficacy in repelling and killing adult mosquitoes to help prevent disease transmission.[76] In agreement with our findings, another study reported that the essential oils of *Citrus aurantium*, *Cymbopogon citratus*, and *Cinnamomum verum* were highly effective in killing both adults and eggs of *A. aegypti* and *A. albopictus*, with *C. verum* oil showing an inhibition rate of 91.0–93.0%.[77] Additionally, a study[78] revealed that clove oil exhibited the highest effectiveness against *A. aegypti* when formulated in coconut and olive oils, providing protection durations of 96.00 and 76.50 minutes, respectively. Likewise, citronella grass oil in coconut oil, citronella grass oil in olive oil, and lemongrass oil in coconut oil afforded protection against *Culex quinquefasciatus* for 165.00, 105.00, and 112.50 minutes, respectively. Their research made it very evident that lemongrass, citronella, and clove oils held the greatest promise for mosquito repellents. However, it has been demonstrated that being essential for stress physiology, GST and acetylcholinesterase (AChE), which protect insects against insecticidal chemicals, are engaged in intracellular transport and several biosynthetic activities.[79] The levels of AChE and GST enzymes were also measured after testing these dyes on *C. pipiens* mosquito larvae to determine their toxicity, where AChE and GST were 40, 39, 38, and 37 and 2.3, 2.3, 2.4, and 2.4 μg eq min^{-1} mg^{-1} protein in the case of **6a–d** compared to 38 and 2.3 μg eq min^{-1} mg^{-1} protein in the control group. The results demonstrated that these dyes exerted no significant effect on the two enzymes with respect to the reference, as illustrated in Fig. 7. In the same context,[80] it was reported that the extract of *Lantana camara* considerably decreased AChE function in larvae compared with those fed on other plant extracts and/or positive controls. These findings support the hypothesis that the *L. camara* extract significantly reduces antioxidant synthesis compared to other plant extracts, which may account for the higher mosquito mortality rate.[81] Furthermore, a previous study[80] demonstrated that the *L. camara* extract exerted the strongest larvicidal effect, likely due to its capacity to suppress GST activity, which enabled its toxic components to disrupt the larval immune system more rapidly than those of other plant extracts.[82] Unlike GST, which was markedly elevated in all examined samples, AChE exhibited variable activity patterns, characterized by a significant increase in response to columbamine and β-sitosterol treatments and a decrease following exposure to AC, palmatine, and jatrorrhizine.[9]

3.5. Docking investigation

3.5.1. Docking on the receptor of AChE (PDB ID: 5x61). The docking protocol was validated by re-docking the co-crystallized

ligand EPE into the enzyme's binding pocket, yielding an energy score (S) of -5.357 kcal mol^{-1}. Molecular docking results revealed that compounds **6a**, **6d**, **6c**, and **6b** exhibited binding energy scores of -8.4233, -7.8642, -7.7104, and -7.427 kcal mol^{-1}, respectively, against the enzyme receptor (PDB ID: 5x61). These values were lower than those of the co-crystallized ligand, suggesting stronger binding affinities, as illustrated in Table 5 and Fig. 8. The greater the engagement, the lower the energy score. As a result, the interaction occurred in the following order: **6a** > **6d** > **6c** > **6b**. The docking outcomes are consistent with the *in vivo* experimental results, further supporting the observed biological activity.

3.5.2. Docking on the receptor of GST (PDB ID: 1pn9). To ensure the reliability of the docking protocol, the co-crystallized ligand (GTX) was re-docked into the enzyme's active site, resulting in an energy score (S) of -5.7243 kcal mol^{-1}, thereby confirming the validity of the docking procedure. Molecular docking analysis revealed that compounds **6d**, **6a**, **6c**, and **6b** exhibited binding energy scores of -6.6624, -6.2752, -6.2494, and -6.0302 kcal mol^{-1}, respectively, against the enzyme receptor (PDB ID: 5X61). These scores were higher than that of the co-crystallized ligand, as shown in Table 6 and Fig. 9. Higher binding affinity corresponds to lower energy scores. Accordingly, the interactions followed the order: **6d** > **6a** > **6c** > **6b**. These results are consistent with the experimental observations from the *in vivo* assay.

4. Conclusions

Our approach to the design and synthesis of four novel disperse dyes involved the confirmation of their chemical compositions. The synthesized dyes were subsequently applied to polyester fabrics in shades 1–5 at temperatures ranging from 100 to 130 °C under various pH conditions (2, 4, 6, 8, and 10). With respect to color levelness and shade depth, the resulting color palette was suitable, exhibiting tones of orange, light brown, reddish brown, and dark brown. High colour strength (13.9, 16.8, 12.2, and 13.9) was achieved by dispersing dyes (**6a, b**, and **d**) under the optimum dyeing conditions of 60 minutes, pH = 2, and 130 °C at a shade level of 3%. These values achieved the required dyeing levelness and shade depth for dyes **6a–d**. Importantly, this study emphasizes optimizing dyeing conditions to achieve the best color outcomes for polyester fabrics using the previously described disperse dyes. This study demonstrated that textile fabrics can be finished with insect-repellent agents to provide external protection against mosquito bites, making them suitable for use in door curtains, military uniforms, bed linens, tablecloths, and sofa covers.

Author contributions

Mohamed S. A. El-Gaby: supervision, conceptualization, and writing. M. A. Habib: supervision, writing and review. Nadeem Raza: preparation of the final research report. Ahmed B. M. Ibrahim: writing. Ali A. Ali: conceptualization, methodology,

data curation, editing, writing, and review. Walid E. Elgammal: conceptualization, methodology, and data curation. Ahmed H. Halawa: resources, data curation, validation, and formal analysis. Mostafa A. Ismail: investigation, resources, and formal analysis. Tharwat A. Selim: biological activity of dyed-fabric samples, methodology, writing, and review. Ahmed I. Hasaballah: biochemical assay, methodology, writing, and review. Mohamed A. M. El-Tabakh: molecular docking software, writing, and review. Gameel A. M. Elhagali: conceptualization and review.

Conflicts of interest

The authors declare that they have no known financial or personal conflicts of interest that could have influenced the work reported in this paper.

Data availability

Data will be made available upon request.

All authors confirm that the data which supporting the findings of this study are available within the article and its supplementary information (SI). Supplementary information: Fig. S1–S20. See DOI: https://doi.org/10.1039/d5ma01162k.

Supplementary data has been deposited with Protein Data Bank: 5x61 and 1PN9.[83a,b]

Acknowledgements

References

1 B. Sartorius, J. Cano, H. Simpson, L. S. Tusting, L. B. Marczak, M. K. Miller-Petrie, B. Kinvi, H. Zoure, P. Mwinzi and S. I. Hay, *Lancet Global Health*, 2021, **9**, e52–e60.

2 T. A. Selim, S. H. Ragab, S. A. Riad, R. I. Eltaly, S. H. Mohammed, S. E. Sharawi, N. A. Alkenani, R. S. Almahallawi, H. S. Al-Rashidi and M. A. El-Tabakh, *Insects*, 2025, **16**, 433.

3 M. M. El-Bahnasawy, L. A. Megahed, H. A. A. Saleh and T. A. Morsy, *J. Egypt. Soc. Parasitol.*, 2013, **43**, 41–56.

4 S. Zotzmann, A. Steinbrink, K. Schleich, F. Frantzmann, C. Xoumpholphakdy, M. Spaeth, C. V. Moro, P. Mavingui and S. Klimpel, *Parasitol. Res.*, 2017, **116**, 1899–1906.

5 M. M. El-Bahnasawy, M. K. M. Khater and T. A. Morsy, *J. Egypt. Soc. Parasitol.*, 2013, **43**, 87–102.

6 A. Gabarty, T. A. Selim and A. I. Hasaballah, *J. Radiat. Res. Appl. Sci.*, 2022, **15**, 1–6.

7 F. I. Abdallah, B. A. Merdan, F. A. Shaarawi, A. F. Mohamed, T. A. Selim, S. M. Dahesh and M. H. Rady, *Beni-Suef Univ. J. Basic Appl. Sci.*, 2024, **13**, 119.

8 A. Hasaballah, T. Selim, M. Tanani and E. Nasr, *Afr. Entomol.*, 2021, **29**, 479–490.

9 T. A. Selim, I. E. Abd-El Rahman, H. A. Mahran, H. A. Adam, V. Imieje, A. A. Zaki, M. A. Bashar, H. Hwihy, A. Hamed and A. A. Elhenawy, *Insects*, 2022, **13**, 676.

10 A. H. Hashem, T. A. Selim, M. H. Alruhaili, S. Selim, D. H. M. Alkhalifah, S. K. Al Jaouni and S. S. Salem, *J. Funct. Biomater.*, 2022, **13**, 112.

11 A. E. Mekky, E. Saied, M. M. Al-Habibi, Z. A. Shouaib, A. I. Hasaballah, M. E. Rashed, A. F. Khaled, A. N. Alshammari, F. S. Youssef and A. M. Al-Shahat, *Sci. Rep.*, 2025, **15**, 27845.

12 S. K. Maguranyi, C. E. Webb, S. Mansfield and R. C. Russell, *J. Am. Mosq. Control Assoc.*, 2009, **25**, 292–300.

13 R. Prabha and R. Vasugi, *Indian J. Sci.*, 2012, **1**, 74–76.

14 U. Agarwal, S. Verma and R. K. Tonk, *Bioorg. Med. Chem. Lett.*, 2024, 129912.

15 M. K. Vanga, R. Bhukya, V. Thumma, V. Tamalapakula, L. S. Boddu and V. Manga, *Chem. Biodiversity*, 2024, **21**, e202401583.

16 Y. Li, T. Ma, Y. Yang, X. Zhong, G. Zhu, J. Wang, W. Chen, J. Fan, L. Tang and W. Liu, *J. Agric. Food Chem.*, 2024, **72**, 26983–26995.

17 X. Yang, D. Liu, C. Wei, J. Li, C. Zhao, Y. Tian, X. Li, B. Song and R. Song, *iScience*, 2024, **27**, 111210.

18 F. F. Alblewi, M. H. Alsehli, Z. M. Hritani, A. Eskandrani, W. H. Alsaedi, M. O. Alawad, A. A. Elhenawy, H. Y. Ahmed, M. S. El-Gaby and T. H. Afifi, *Int. J. Mol. Sci.*, 2023, **24**, 16716.

19 R. M. Okasha, M. Alsehli, S. Ihmaid, S. S. Althagfan, M. S. El-Gaby, H. E. Ahmed and T. H. Afifi, *Bioorg. Chem.*, 2019, **92**, 103262.

20 N. Cai, X. Gao, L. Jia, Y. Liu, J. Zhao, J. Qu and Y. Zhou, *Bioorg. Chem.*, 2025, **154**, 108050.

21 S. Abdolmohammadi and B. Mirza, *Results Chem.*, 2025, 102060.

22 M. T. Chen, H. Y. Chen, Y. F. Luo, J. Zhou, J. J. Yang, Z. P. Jiang and L. Huang, *Chem. Biodiversity*, 2024, e202402465.

23 D. Sangeetha, *J. Mol. Struct.*, 2025, **1322**, 140562.

24 M. Z. Saif, N. J. I. Esha, S. T. Quayum, S. Rahman, M. A. Al-Gawati, G. Alsowygh, H. Albrithen, A. N. Alodhayb, R. A. Poirier and K. M. Uddin, *Sci. Rep.*, 2024, **14**, 13221.

25 B. N. Sudha, V. G. Sastry, M. S. Harika and N. Yellasubbaiah, *Indian J. Chem.*, 2018, **57**, 737–745.

26 M. Saeedi, M. Safavi, E. Karimpour-Razkenari, M. Mahdavi, N. Edraki, F. H. Moghadam, M. Khanavi and T. Akbarzadeh, *Bioorg. Chem.*, 2017, **70**, 86–93.

27 W. Yuanhui, L. Na, H. Jincai, L. Hao, L. Zuren, L. Dingfeng and B. Lianyang, *Chin. J. Pestic. Sci.*, 2024, **26**, 857–869.

28 W. Zhao, B. Wang, Y. Liu, L. Fu, L. Sheng, H. Zhao, Y. Lu and D. Zhang, *Eur. J. Med. Chem.*, 2020, **189**, 112075.

29 K. Mezgebe and E. Mulugeta, *RSC Adv.*, 2022, **12**, 25932–25946.

30 E. El-Sayed, A. El-Aziz, H. Othman and A. G. Hassabo, *Egypt. J. Chem.*, 2024, **67**, 87–97.

31 S. Benkhaya, S. M'rabet and A. El Harfi, *Heliyon*, 2020, **6**, e03271.

32 F. Hamon, F. Djedaini-Pilard, F. Barbot and C. Len, *Tetrahedron*, 2009, **65**, 10105–10123.

33 C. Patil, D. S. Talele, S. P. Talele, P. R. Pohekar and D. Kolhe, *J. Pharm. Sci. Res.*, 2019, **11**, 2213–2219.

34 B. Zhang, L. Song, C. Feng and W. Tian, *ChemistrySelect*, 2022, **7**, e202203948.

35 C. Lei, W. Yang, Z. Lin, Y. Tao, R. Ye, Y. Jiang, Y. Chen and B. Zhou, *RSC Adv.*, 2024, **14**, 20339–20350.

36 T. Marinov, Z. Kokanova-Nedialkova and P. T. Nedialkov, *Diversity*, 2023, **15**, 1030.

37 K. Surana, B. Chaudhary, M. Diwaker and S. Sharma, *Med-ChemComm*, 2018, **9**, 1803–1817.

38 S. Sheng Zhu, X. Li Liu, P. Fei Liu, Y. Li, J. Qiang Li, H. Min Wang, S. Kui Yuan and N. Guo Si, *Phytopathology*, 2007, **97**, 643–649.

39 M. C. Cuquerella, V. Lhiaubet-Vallet, J. Cadet and M. A. Miranda, *Acc. Chem. Res.*, 2012, **45**, 1558–1570.

40 J. Leegwater-Kim and C. Waters, *Expert Rev. Neurother.*, 2007, **7**, 1649–1657.

41 R. S. Rosenson, *Expert Rev. Cardiovasc. Ther.*, 2008, **6**, 1319–1330.

42 K. Sivakumar and A. Nalini, *J. Mol. Liq.*, 2024, **395**, 123905.

43 M. El-Gaby, A. Atalla, A. Gaber and K. Abd Al-Wahab, *Il Farmaco*, 2000, **55**, 596–602.

44 M. S. El-Gaby, N. M. Taha, J. A. Micky and M. A. El-Sharief, *Acta Chim. Slov.*, 2002, **49**, 159–171.

45 N. M. Saleh, M. S. El-Gaby, K. El-Adl and N. E. Abd El-Sattar, *Bioorg. Chem.*, 2020, **104**, 104350.

46 A. M. Sayed, F. A. Taher, M. R. Abdel-Samad, M. S. El-Gaby, K. El-Adl and N. M. Saleh, *Bioorg. Chem.*, 2021, **108**, 104669.

47 M. El-Gaby, M. Hussein, M. A. Reheim, A. Abdou, A. Fahmy, A. Drar and M. Gad, *Russ. J. Bioorg. Chem.*, 2024, **50**, 917–933.

48 M. El-Gaby, G. E.-H. Ali, M. A. Reheim, A. Abdou, M. Bakry, A. Drar and M. Gad, *Russ. J. Bioorg. Chem.*, 2024, **50**, 1037–1048.

49 M. El-Gaby, M. Hussein, F. Faraghally, A. Drar and M. Gad, *Curr. Chem. Lett.*, 2023, **12**, 599–606.

50 A. A. Ali, M. Abass, S. El-Molla, S. A. Halim and E.-S. Ibrahim, *Pigm. Resin Technol.*, 2024, **53**, 1017–1027.

51 S. Yoon, B. Choi, M. M. Rahman, S. Kumar, S. M. Mamun Kabir and J. Koh, *Materials*, 2019, **12**, 4209.

52 A. A. Ali, H. Abd El-Wahab, M. S. Abusaif, A. Ragab, O. A. Abdel-Jaid, E. Eldeeb and Y. A. Ammar, *Pigm. Resin Technol.*, 2024, **53**, 557–568.

53 A. A. Ali, M. M. Elsawy, S. S. Salem, A. A. El-Henawy and H. Abd El-Wahab, *Pigm. Resin Technol.*, 2023, **52**, 19–32.

54 A. A. Ali, M. Alshukur, A. M. Ashmawy, A. M. Mahmoud, A. Saleh, H. S. Nassar and B. Yao, *Res. J. Text. Apparel*, 2024, **28**, 478–492.

55 M. Larvicides, *Google Scholar*, 2005.

56 D. Simpson, D. Bull and D. Lindquist, *Ann. Entomol. Soc. Am.*, 1964, **57**, 367–371.

57 C.-H. Kao, C.-F. Hung and C.-N. Sun, *J. Econ. Entomol.*, 1989, **82**, 1299–1304.

58 W. S. Abbott, *J. Econ. Entomol.*, 1925, **18**, 265–267.

59 A. A. Ali, M. A. Ismail, W. E. Elgammal, A. Belal, A. J. Obaidullah, A. K. Khalil, G. A. Elhagali and M. S. El-Gaby, *Sci. Rep.*, 2025, **15**, 4360.

60 J. Chen, L. Pei, W. Shi, J. Yi and J. Wang, *Polymers*, 2023, **15**, 1046.

61 A. A. Ali, M. Elsawy, N. M. Saleh, A. A. El-Henawy, F. A. M. Al-Zahrani and H. A. El-Wahab, *Pigm. Resin Technol.*, 2025.

62 N. H. Bahtiti, W. E. Elgammal, A. A. Ali, A. Belal, O. Abdullah, M. M. Ghoneim, M. S. Qenawy and M. M. Abdou, *ACS Omega*, 2023, **9**, 447–455.

63 M. M. Abdou, A. A. Ali, H. A. El-Wahab, H. F. Al Shareef and F. A. Al-Zahrani, *Fibers Polym.*, 2024, 1–16.

64 S. S. Pawar, S. Maiti, S. Biranje, K. Kulkarni and R. V. Adivarekar, *Heliyon*, 2019, **5**, e01606.

65 W. E. Elgammal, A. A. Ali, A. E. Hassan, F. A. M. Al-Zahrani, E. K. Alenezy and H. A. El-Wahab, *ACS Omega*, 2025, **10**, 6876–6890.

66 A. A. Ali, F. A. M. Al-Zahrani, W. E. Elgammal, M. Ali, A. M. Mahmoud and H. Abd El-Wahab, *Pigm. Resin Technol.*, 2025, **54**, 982–993.

67 O. A. A. Ali, H. F. Al Shareef, R. Felaly, A. A. Ali, M. Elsawy, A. Belal, R. I. Alsantali, A. B. Mehany, S. Al-Shomar and N. Abdelshafi, *J. Mol. Struct.*, 2025, **1337**, 142075.

68 W. E. Elgammal, A. A. Ali, G. A. Elhagali, M. A. Ismail, A. Belal, N. K. Albezrah, M. A. Ali, M. A. El-Tabakh, M. A. Alrayyani and M. S. El-Gaby, *ACS Omega*, 2025, **10**, 39567–39579.

69 O. A. Abu Ali, A. A. Ali, N. M. Saleh, M. Elsawy, A. A. El-Henawy and H. Abd El-Wahab, *Chem. Afr.*, 2025, **8**, 995–1014.

70 A. M. Lutambi, M. A. Penny, T. Smith and N. Chitnis, *Math. Biosci.*, 2013, **241**, 198–216.

71 R. Mia, M. Selim, A. Shamim, M. Chowdhury, S. Sultana, M. Armin, M. Hossain, R. Akter, S. Dey and H. Naznin, *J. Text. Eng. Fashion Technol.*, 2019, **5**, 220–226.

72 M. D. Teli and P. P. Chavan, *J. Text. Inst.*, 2018, **109**, 427–434.

73 D. Saber and K. Abd El-Aziz, *J. Ind. Text.*, 2022, **51**, 246S–271S.

74 M. M. Baz, A. S. Montaser and R. M. Ali, *J. Text. Inst.*, 2025, **116**, 293–308.

75 M. Soonwera and S. Sittichok, *Environ. Sci. Pollut. Res.*, 2020, **27**, 20201–20214.

76 M.-X. Li, Y.-P. Ma, H.-X. Zhang, H.-Z. Sun, H.-H. Su, S.-J. Pei and Z.-Z. Du, *Plant Diversity*, 2021, **43**, 317–323.

77 T. Moungthipmalai, C. Puwanard, J. Aungtikun, S. Sittichok and M. Soonwera, *Sci. Rep.*, 2023, **13**, 2119.

78 M. Sharififard, I. Alizadeh, E. Jahanifard, C. Wang and M. E. Azemi, *J. Arthropod.-Borne Dis.*, 2018, **12**, 387.

79 M. T. Rehman, M. F. AlAjmi, A. Hussain, G. M. Rather and M. A. Khan, *Int. J. Mol. Sci.*, 2019, **20**, 819.

80 H. M. Al-Solami, *J. King Saud Univ., Sci.*, 2021, **33**, 101371.

81 N. Abutaha, F. A. Al-Mekhlafi, L. A. Al-Keridis, M. Farooq, F. A. Nasr and M. Al-Wadaan, *Entomol. Res.*, 2018, **48**, 362–371.

82 İ. Gulçin, P. Taslimi, A. Aygün, N. Sadeghian, E. Bastem, O. I. Kufrevioglu, F. Turkan and F. Şen, *Int. J. Biol. Macromol.*, 2018, **119**, 741–746.

83 (*a*) Q. Han, D. M. Wong, H. Robinson, H. Ding, P. C. H. Lam, M. M. Totrov, P. R. Carlier and J. Li, Crystal structure of acetylcholinesterase catalytic subunits of the malaria vector Anopheles gambiae, *Insect Sci*, 2017, DOI: 10.1111/1744-7917.12450; (*b*) L. Chen, P. R. Hall, X. E. Zhou, H. Ranson, J. Hemingway and E. J. Meehan, Crystal structure of an insect delta-class glutathione S-transferase from a DDT-resistant strain of the malaria vector Anopheles gambiae, *Acta Crystallogr D Biol Crystallogr*, 2003, **59**, 2211–2217.